EMR'23, Lille (France)

http://emrwebsite.org

« EMR Modelling and Longitudinal Motion Control of a Dual-Motor EVs »

An-Toan NGUYEN[1], Binh-Minh NGUYEN[2], João Pedro F. TROVÃO[1,3], Minh C. TA[1]

[1]University of Sherbooke, Qc, Canada;
[2]University of Tokyo, Tokyo, Japan;
[3]IPC-ISEC and INESC Coimbra, Portugal

« STUDIED ELECTRIC VEHICLE »

e-Commander at e-TESC Lab.

Original topology

Only has one Induction Motor (IM) which is mounted on the front axle for driving four wheels

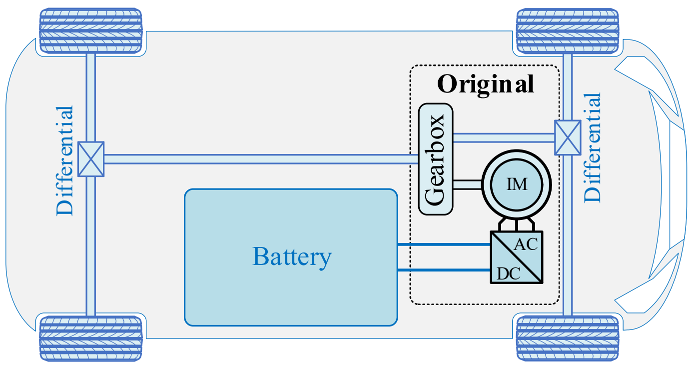

New setup

New dual-motor all-wheel drive by **adding one PMSM** (Permanent Magnet Synchronous Motor)

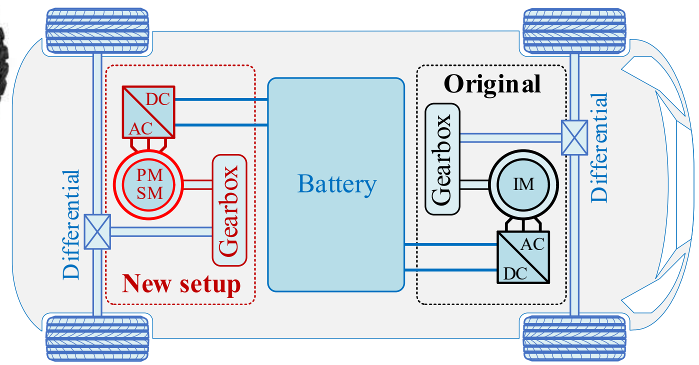

Disadvantages of one-motor all-wheel drive

- Axes are not independent
- Not flexible
- Slow acceleration

Advantages of dual-motor all-wheel drive

- Independent control of each axle
- Flexible operability with three modes
- Powerful, fast and stable acceleration

↳ **How to modelize and control this new configuration ?**

« MODELLING AND CONTROL »

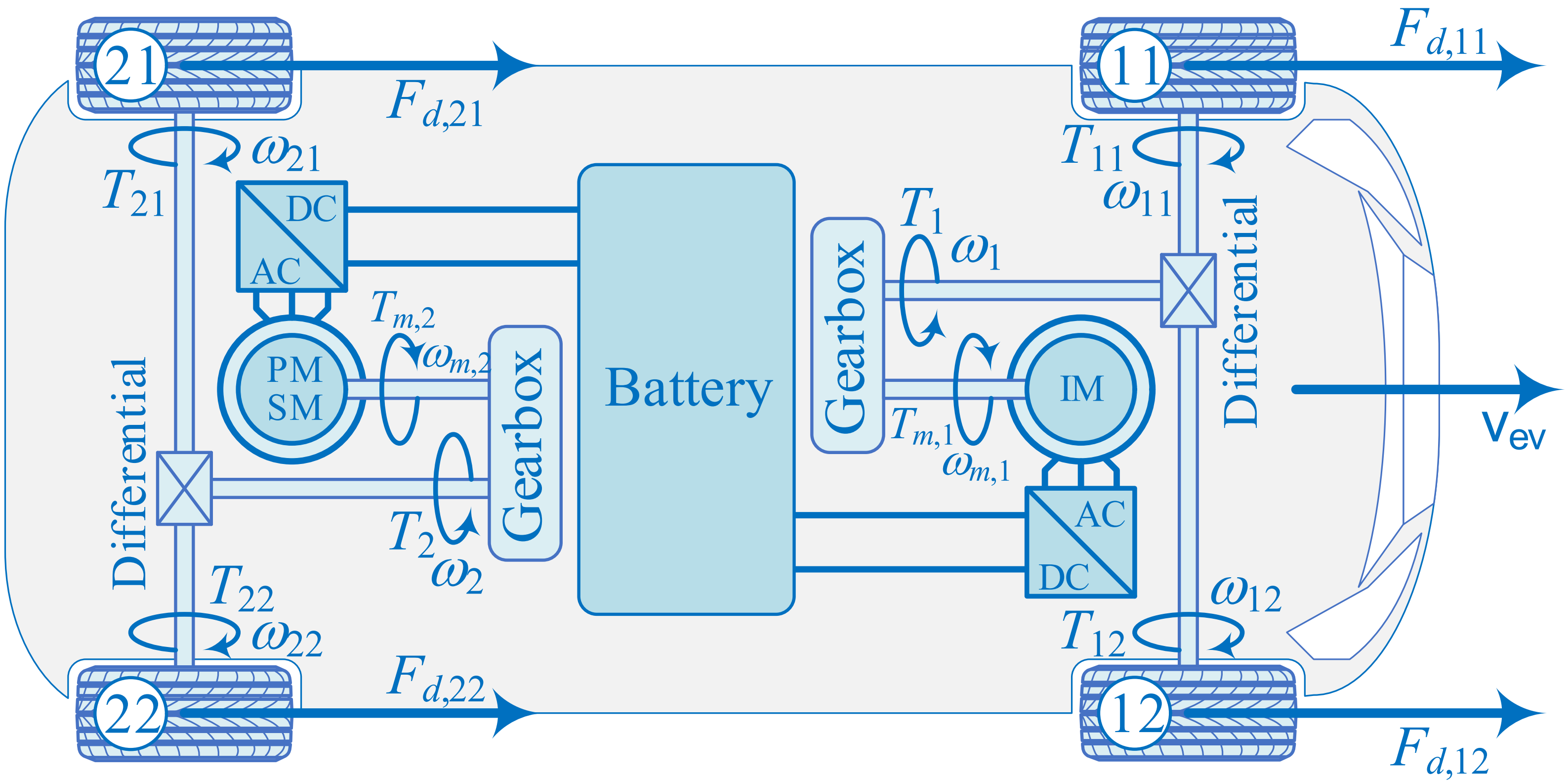

Configuration of the studied dual-motor AWD-EV

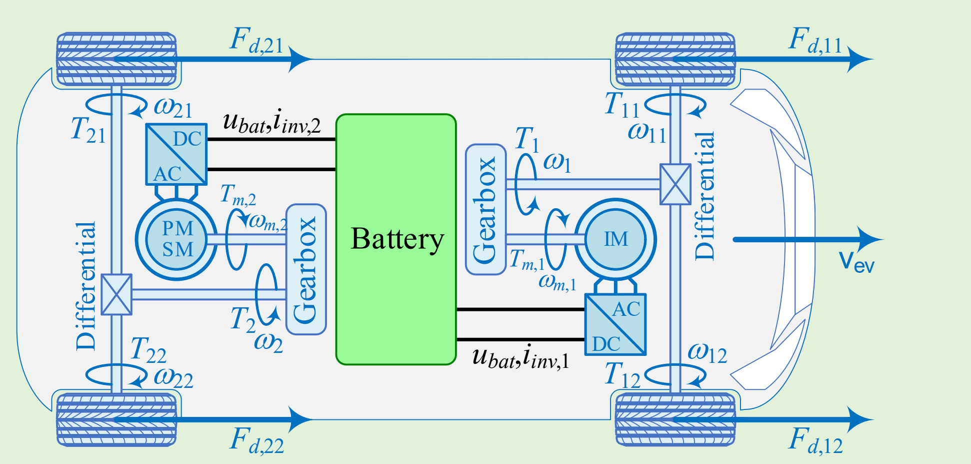

Configuration of the studied dual-motor AWD-EV

1) Battery

$$
\begin{cases}
u_{cell} = u_{cell,OC}(SoC) - r_{cell} i_{cell} \\
SoC_{cell} = SoC_{cell}(0) - \dfrac{1}{C_{eq}} \displaystyle\int_0^t i_{cell} \mathrm{d}t
\end{cases}
\quad (1)
$$

$$
\begin{cases}
u_{bat} = u_{cell} n_s \\
i_{cell} = \dfrac{i_{bat}}{n_p}
\end{cases}
\quad (2)
$$

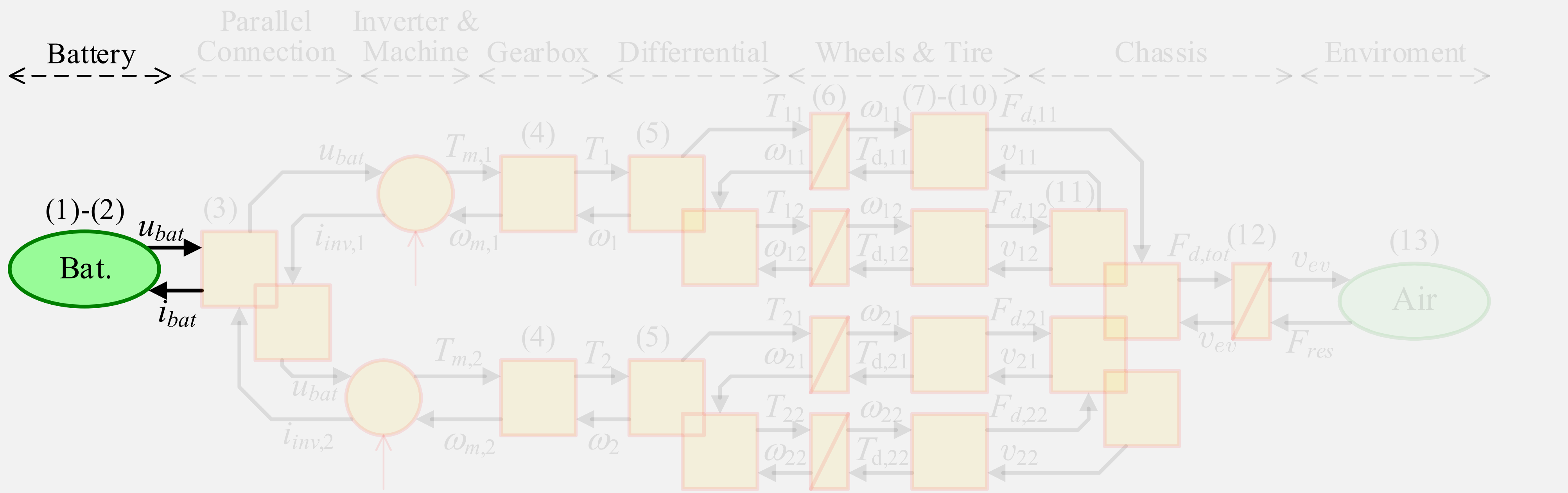

Energetic Macroscopic Representention

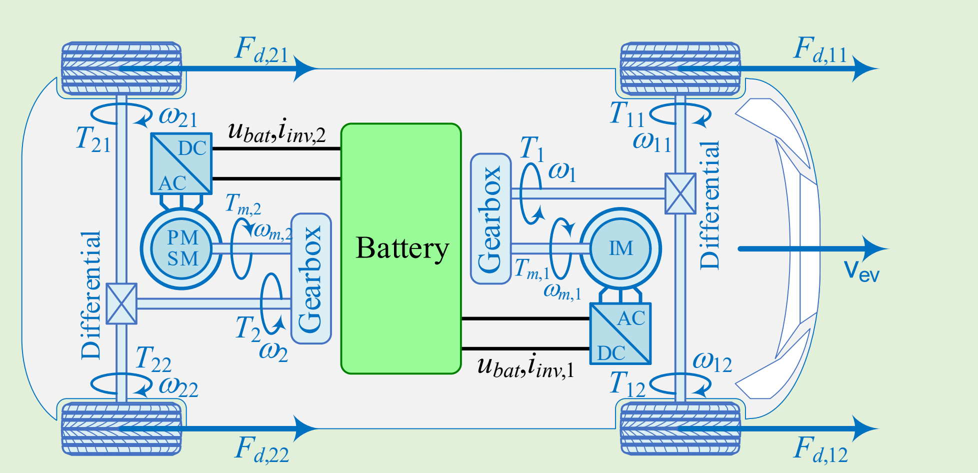

Configuration of the studied dual-motor AWD-EV

1) Battery

$$\begin{cases} u_{bat} \text{ common} \\ i_{bat} = \sum_{i=1}^{2} i_{inv,i} \end{cases} \quad (3)$$

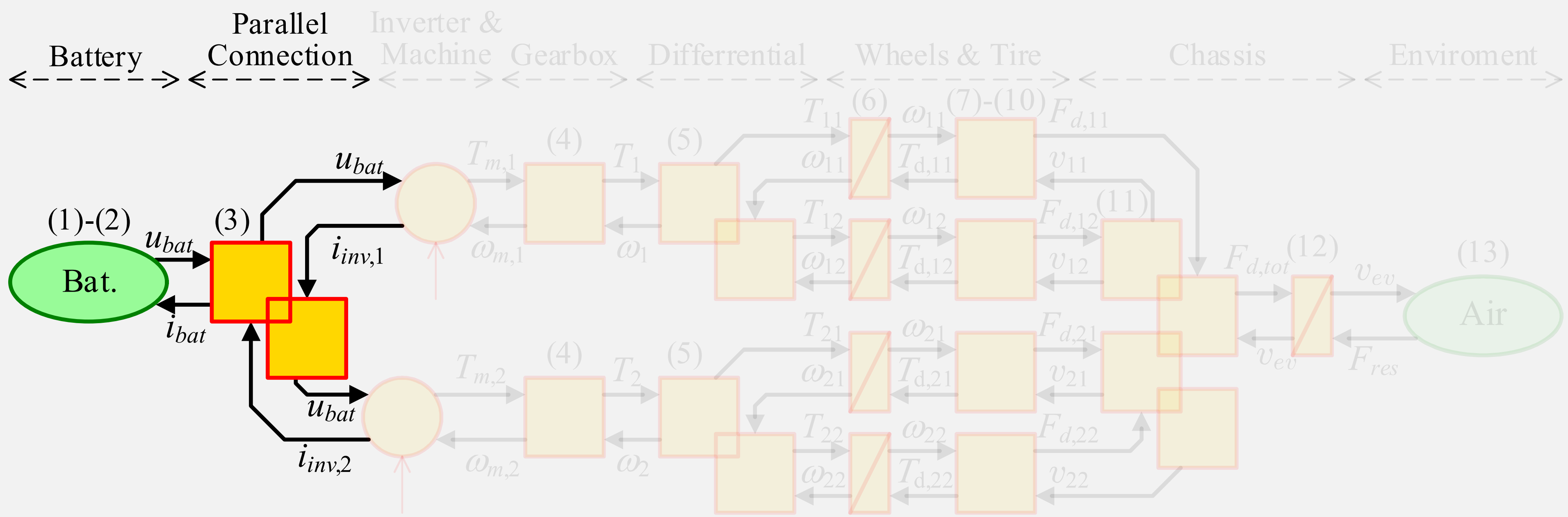

Energetic Macroscopic Represention

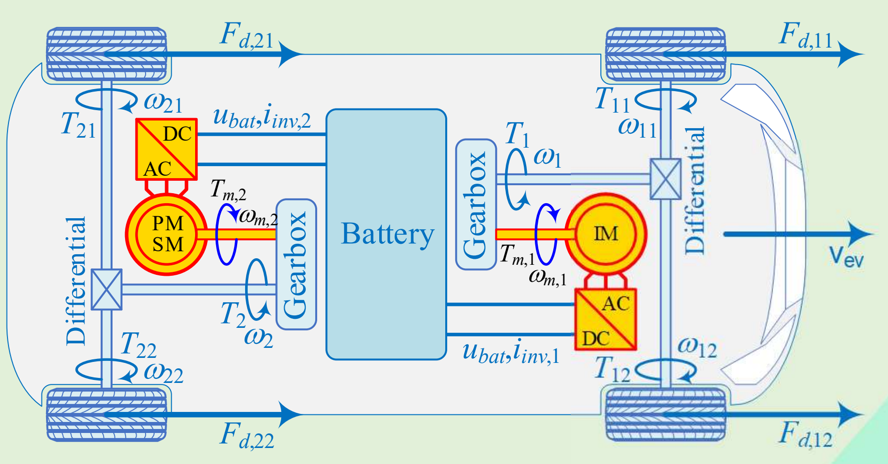

Configuration of the studied dual-motor AWD-EV

3) Inverter and Electric Motor

Dynamic model by EMR

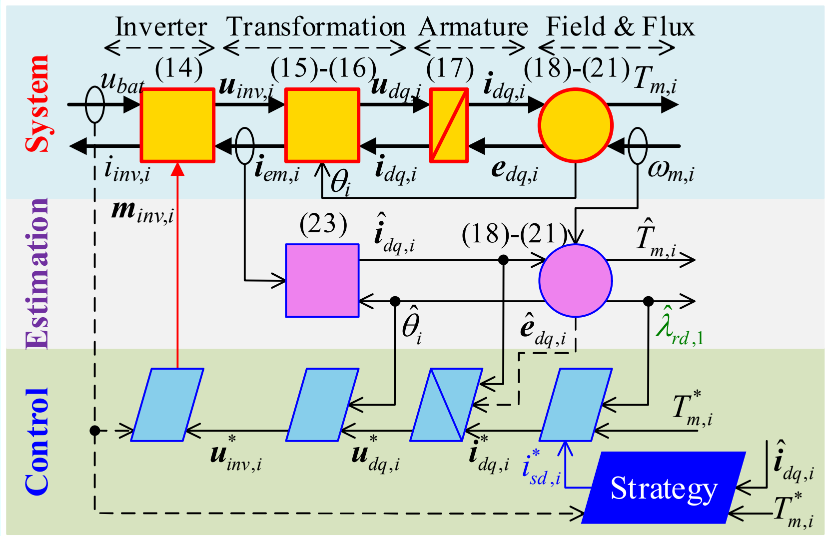

A.-T. Nguyen, B.-M. Nguyen, J. P. F. Trovão, M. C. Ta, "Modelling and Control of Dual-Motor AWD EVs using EMR," CSME – CFD-SC2023, Canada, 2023.

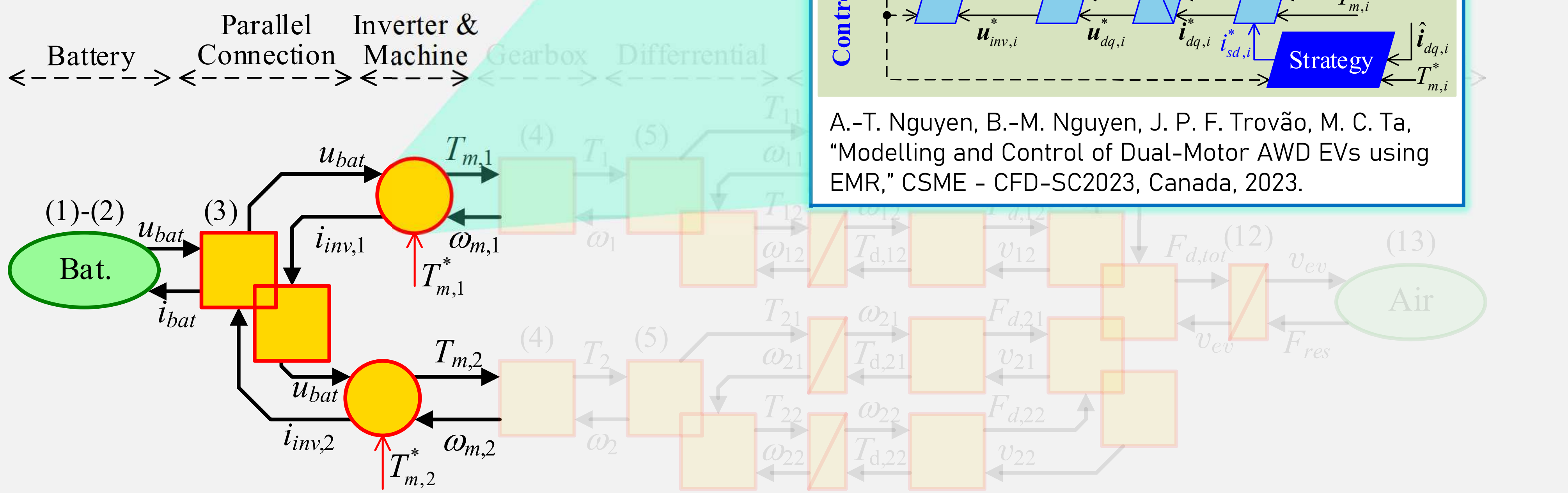

Energetic Macroscopic Represention

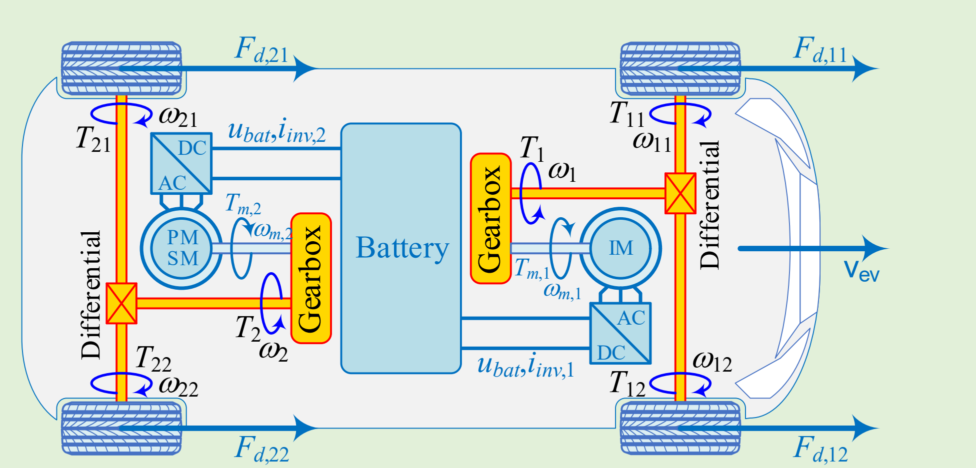

Configuration of the studied dual-motor AWD-EV

4) Gearbox

$$\begin{cases} T_i = k_{gb,i} T_{m,i} \eta_{gb,i}^{k_{tr,i}} \\ \omega_{m,i} = k_{gb,i} \omega_i \end{cases}, \text{ with } k_{tr,i} = \begin{cases} 1 & \text{if } T_i \omega_i \geq 0 \\ -1 & \text{if } T_i \omega_i < 0 \end{cases} \tag{4}$$

5) Differential

$$\begin{cases} T_{ij} = k_{dif,ij} T_i \eta_{dif,i}^{k_{tr,i}} \\ \omega_i = k_{dif,ij} \omega_{ij} \end{cases} \tag{5}$$

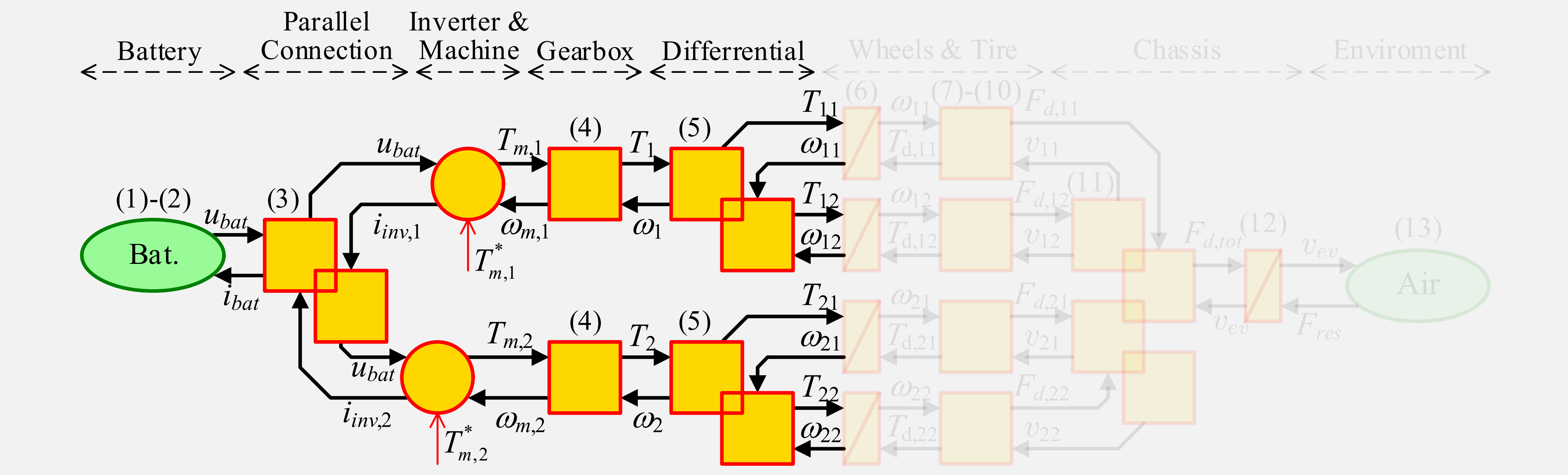

Energetic Macroscopic Represention

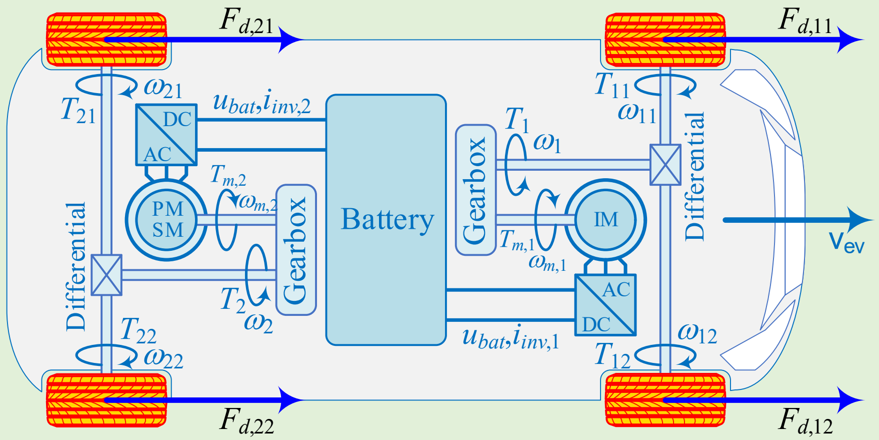

Configuration of the studied dual-motor AWD-EV

6) Wheel & Tire

$$\omega_{ij} = \frac{1}{\widetilde{J}_{\omega,ij}} \int_0^t (T_{ij} - T_{d,ij})\mathrm{d}t \quad (6)$$

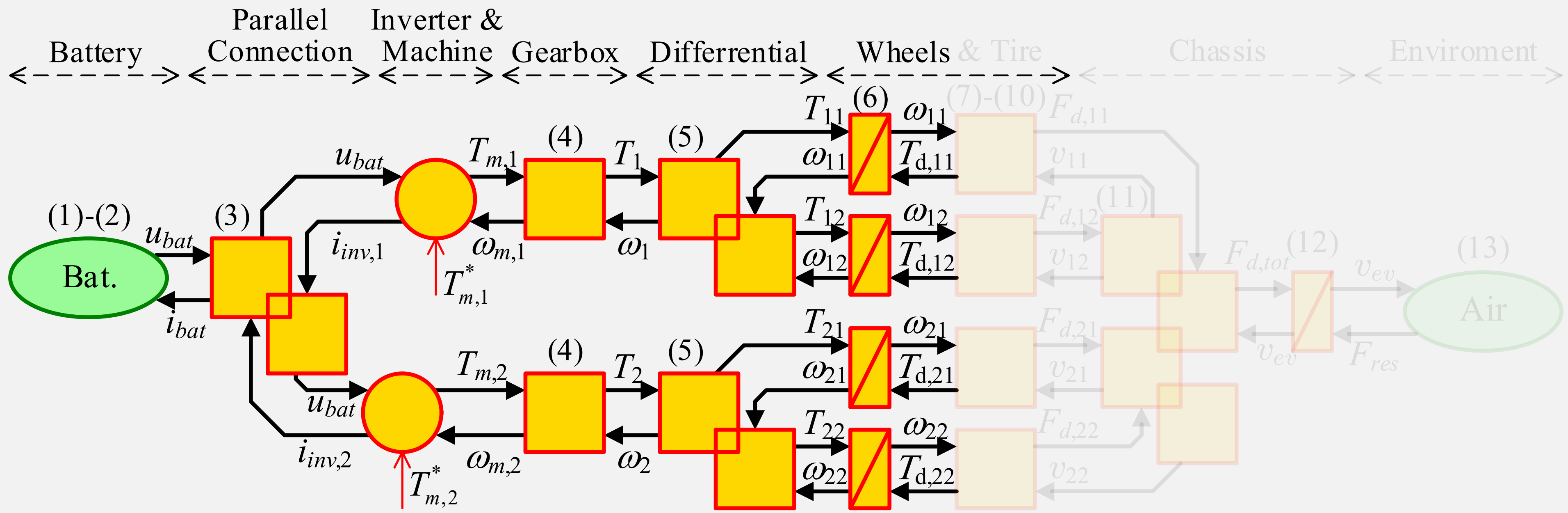

Energetic Macroscopic Represention

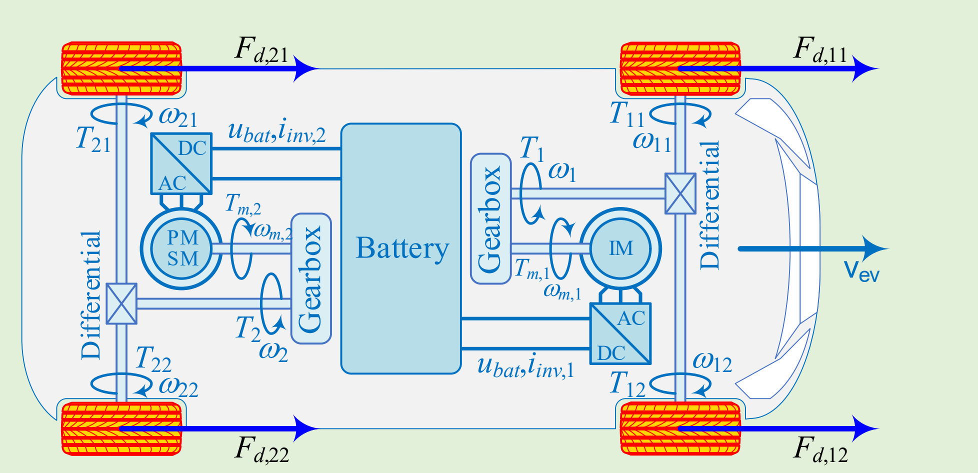

Configuration of the studied dual-motor AWD-EV

6) Wheel & Tire

$$F_{d,ij} = \mu_{ij} F_{z,ij} \sin\left\{C \arctan\left[B\lambda_{ij} - E\left(B\lambda_{ij} - \arctan(B\lambda_{ij})\right)\right]\right\} \quad (7)$$

$$F_{z,ij} = mg\frac{l_i}{2l} + ma\frac{k_x h_{CG}}{2l} \quad (8)$$

$$\lambda_{ij} = \frac{\Delta v_{ij}}{\max\left(R_{wh,ij}\omega_{ij}, v_{ev}, \varepsilon\right)} \quad (9)$$

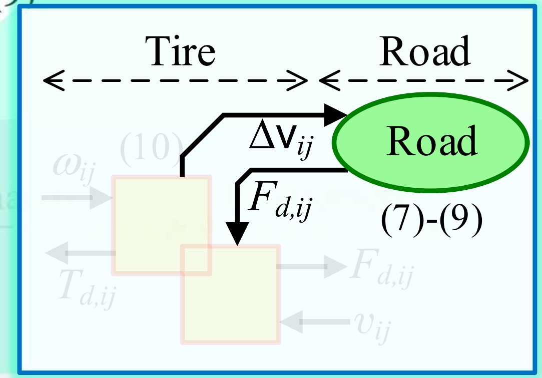

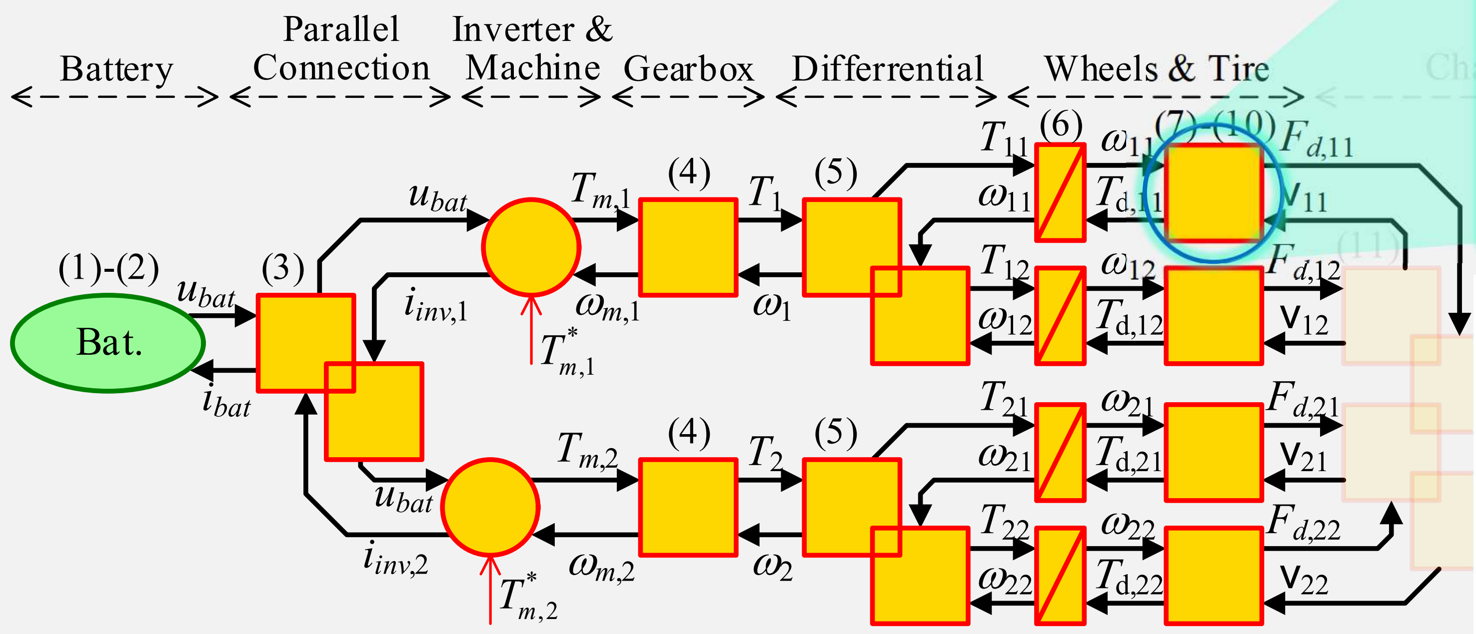

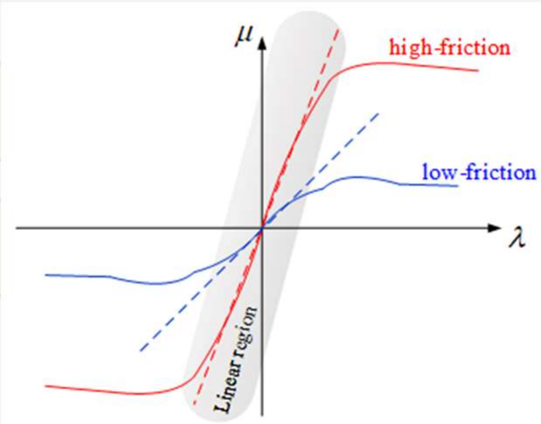

Energetic Macroscopic Represention

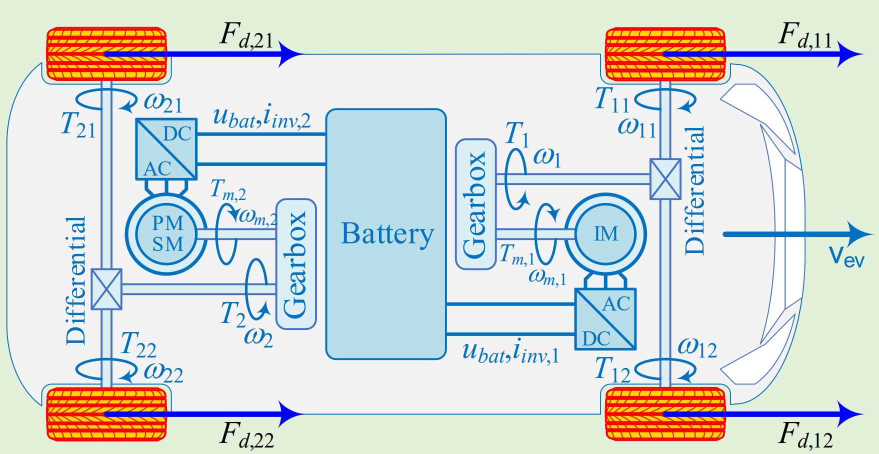

Configuration of the studied dual-motor AWD-EV

6) Wheel & Tire

$$\begin{cases} \Delta v_{ij} = R_{wh,ij}\omega_{ij} - v_{ev} \\ T_{d,ij} = R_{wh,ij}F_{d,ij} \end{cases} \tag{10}$$

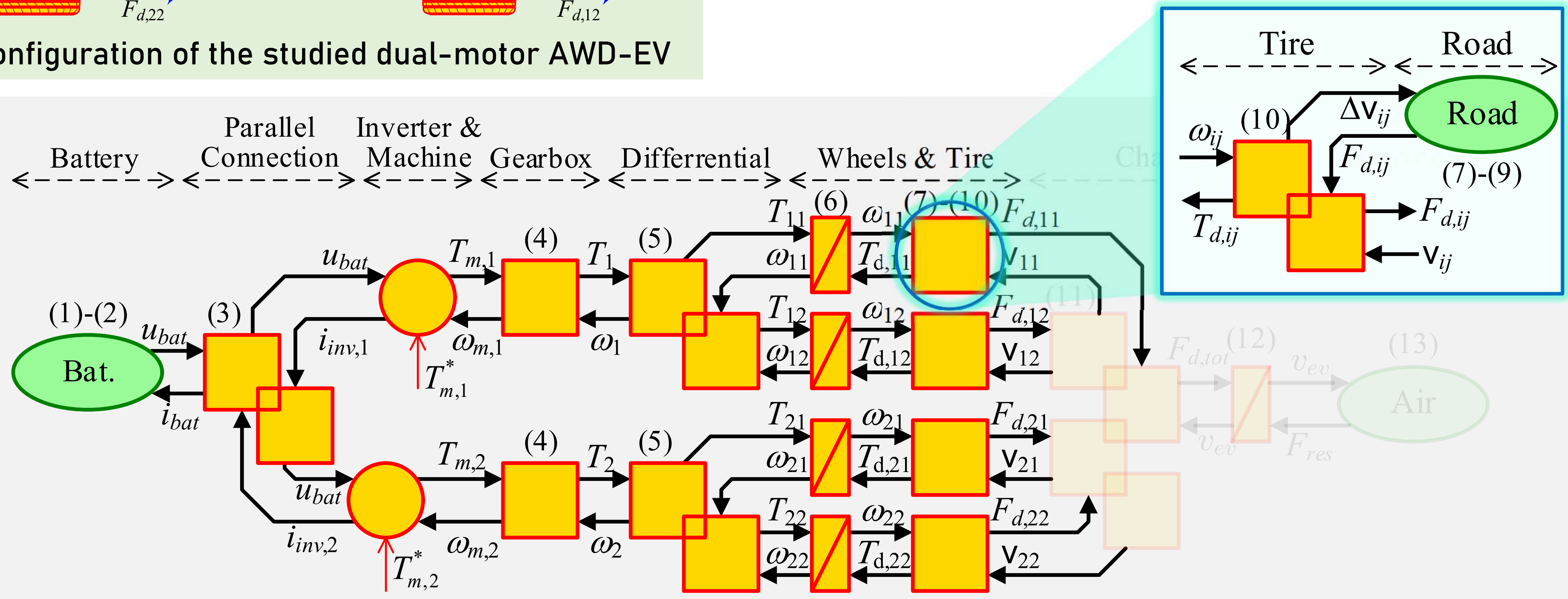

Energetic Macroscopic Represention

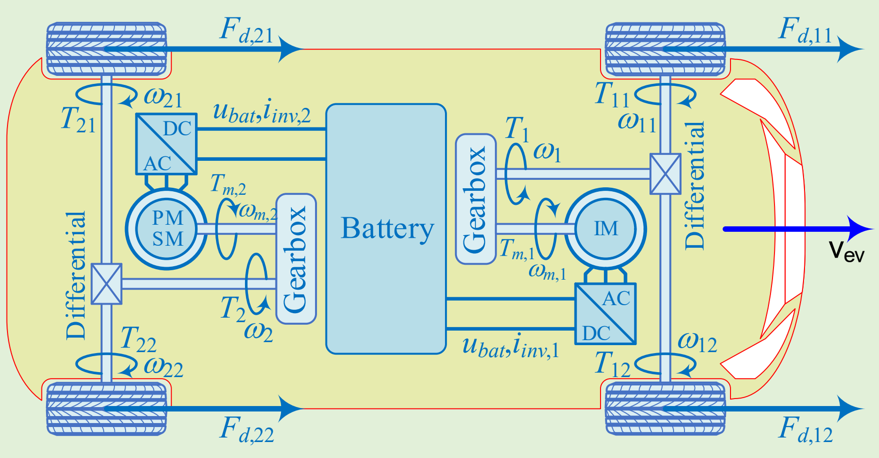

Configuration of the studied dual-motor AWD-EV

7) Chassis

$$\begin{cases} F_{d,tot} = \sum_{i=1}^{2}\sum_{j=1}^{2} F_{d,ij} \\ v_{ij} = v_{ev} \end{cases} \quad (11)$$

$$v_{ev} = \frac{1}{m}\int_0^t (F_{d,tot} - F_{res})\mathrm{d}t \quad (12)$$

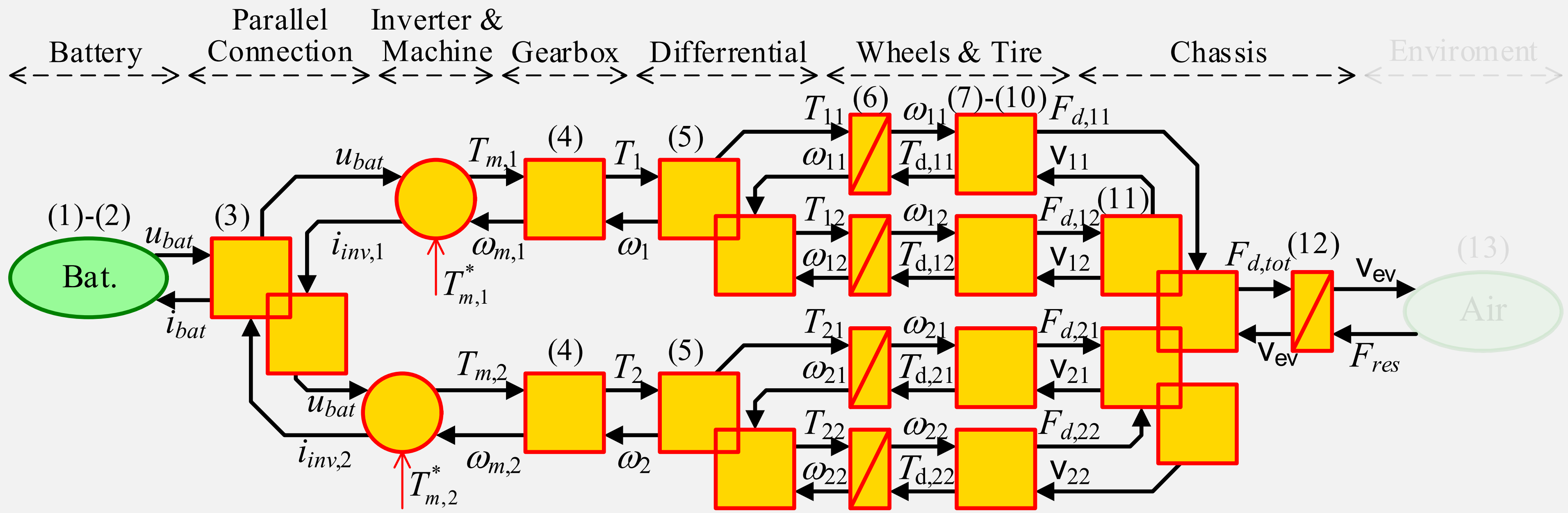

Energetic Macroscopic Represention

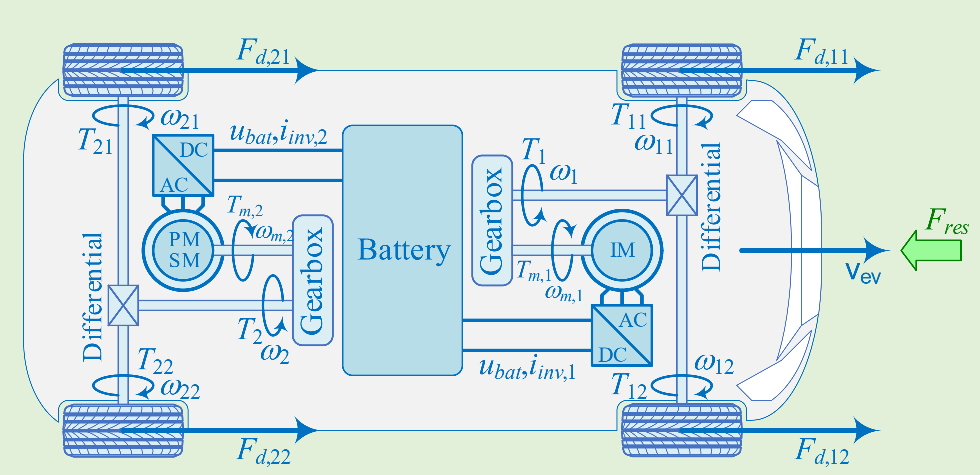

Configuration of the studied dual-motor AWD-EV

8) Environment

$$F_{res} = k_{roll} mg \cos\alpha + 0.5 \rho c_d A_x (v_{ev} + v_{wind})^2 + mg \sin\alpha \quad (13)$$

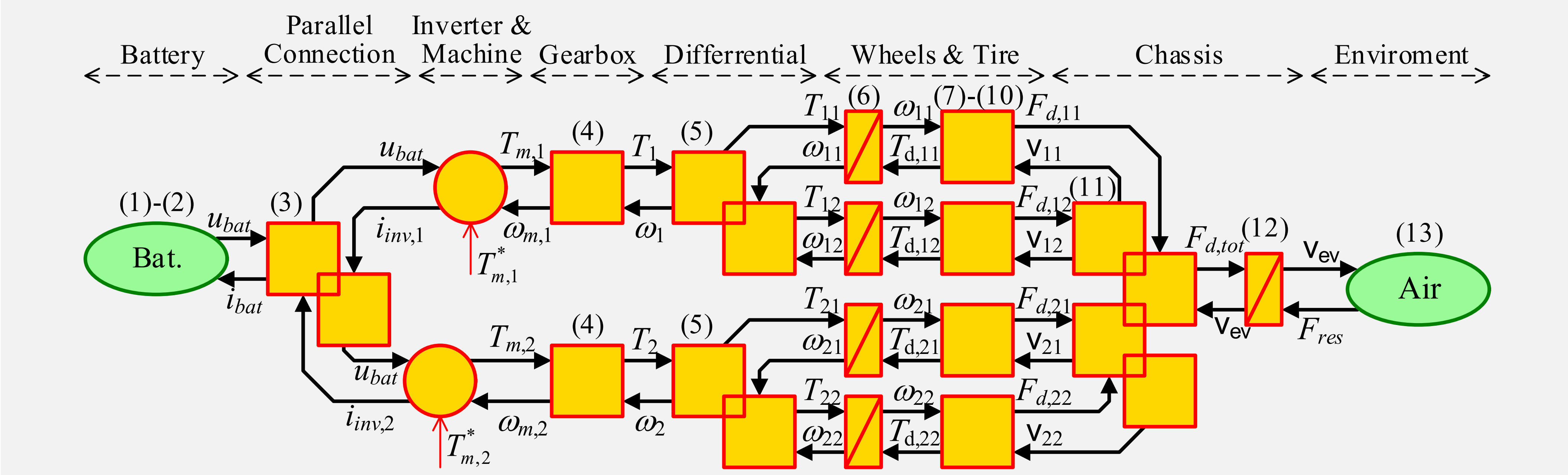

Energetic Macroscopic Represention

EMR and Control of a Dual-Motor Electric Vehicles

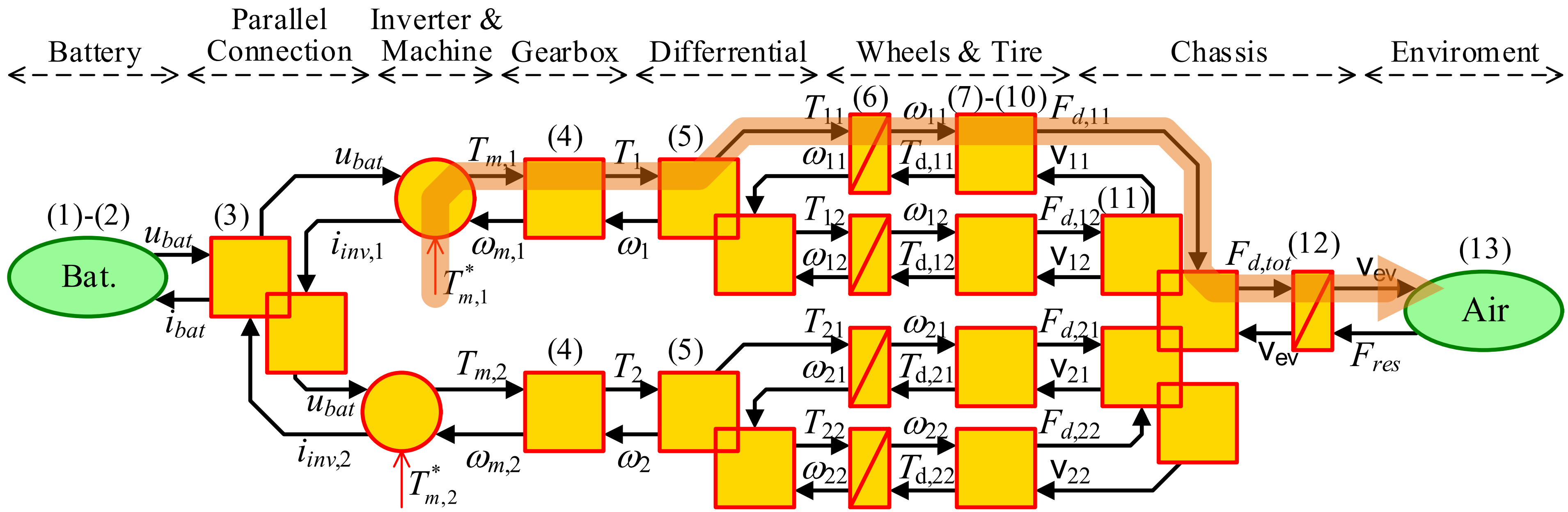

Tuning path

$$T_{m,i} \rightarrow T_i \rightarrow T_{ij} \rightarrow \omega_{ij} \rightarrow F_{d,ij} \xrightarrow{\Sigma} F_{d,tot} \rightarrow v_{ev}$$

$$T^*_{m,i} \leftarrow T^*_i \leftarrow T^*_{ij} \leftarrow \omega^*_{ij} \leftarrow F^*_{d,ij} \leftarrow F^*_{d,tot} \leftarrow v^*_{ev}$$

Control path

1) PI velocity controller

$$F^{*}_{d,tot} = \hat{F}_{res} + k_{I,v}\int_{0}^{t}(v^{*}_{ev} - v_{ev})\mathrm{d}t - k_{P,v}(v^{*}_{ev} - v_{ev}) \quad (24)$$

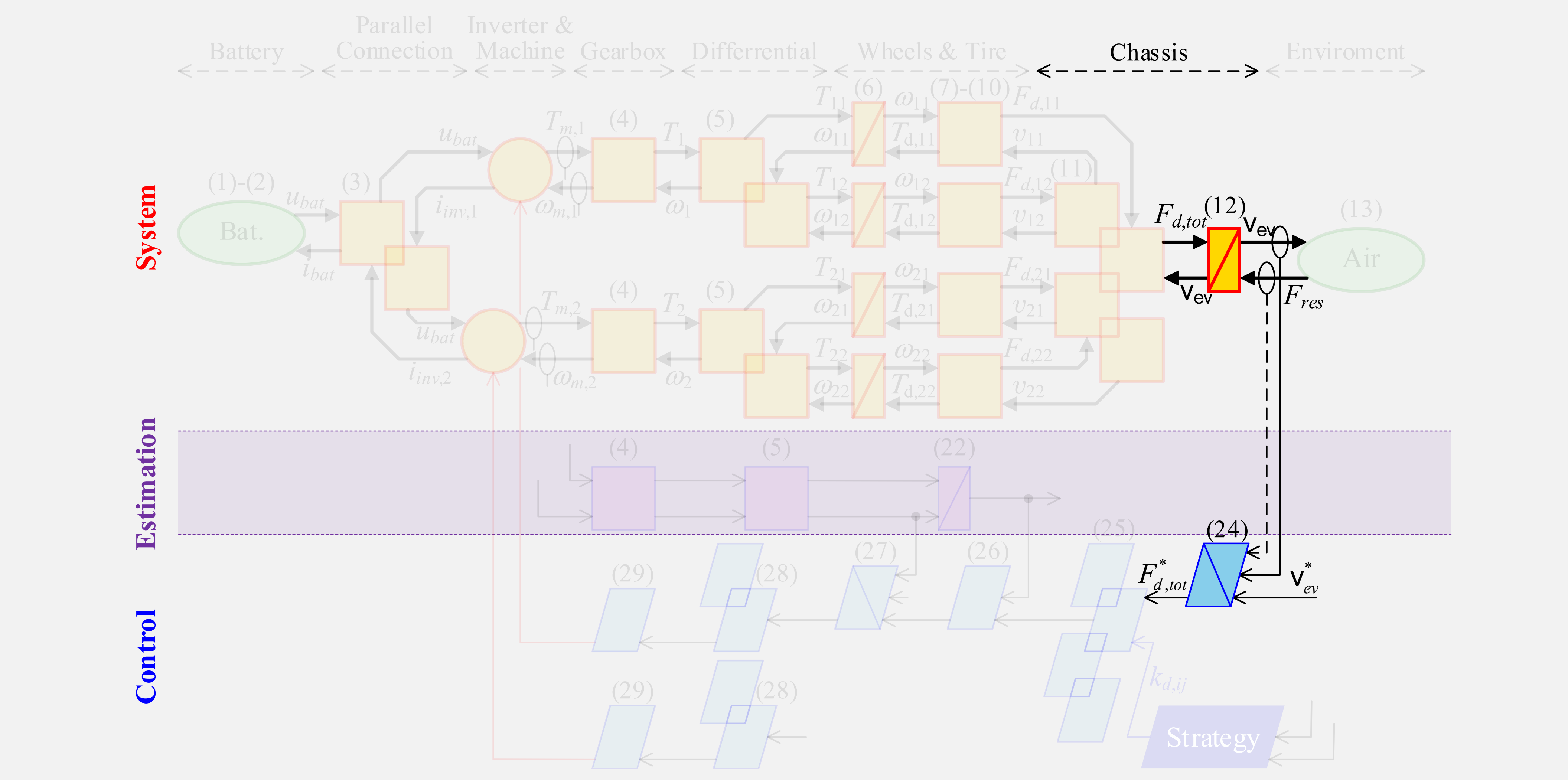

Inversion-Based Control

EMR and Control of a Dual-Motor Electric Vehicles

2) Reference traction forces of each wheel

$$F^*_{d,ij} = k_{d,ij} F^*_{d,tot}, \text{ with } \sum_{i=1}^{2}\sum_{j=1}^{2} k_{d,ij} = 1 \qquad (25)$$

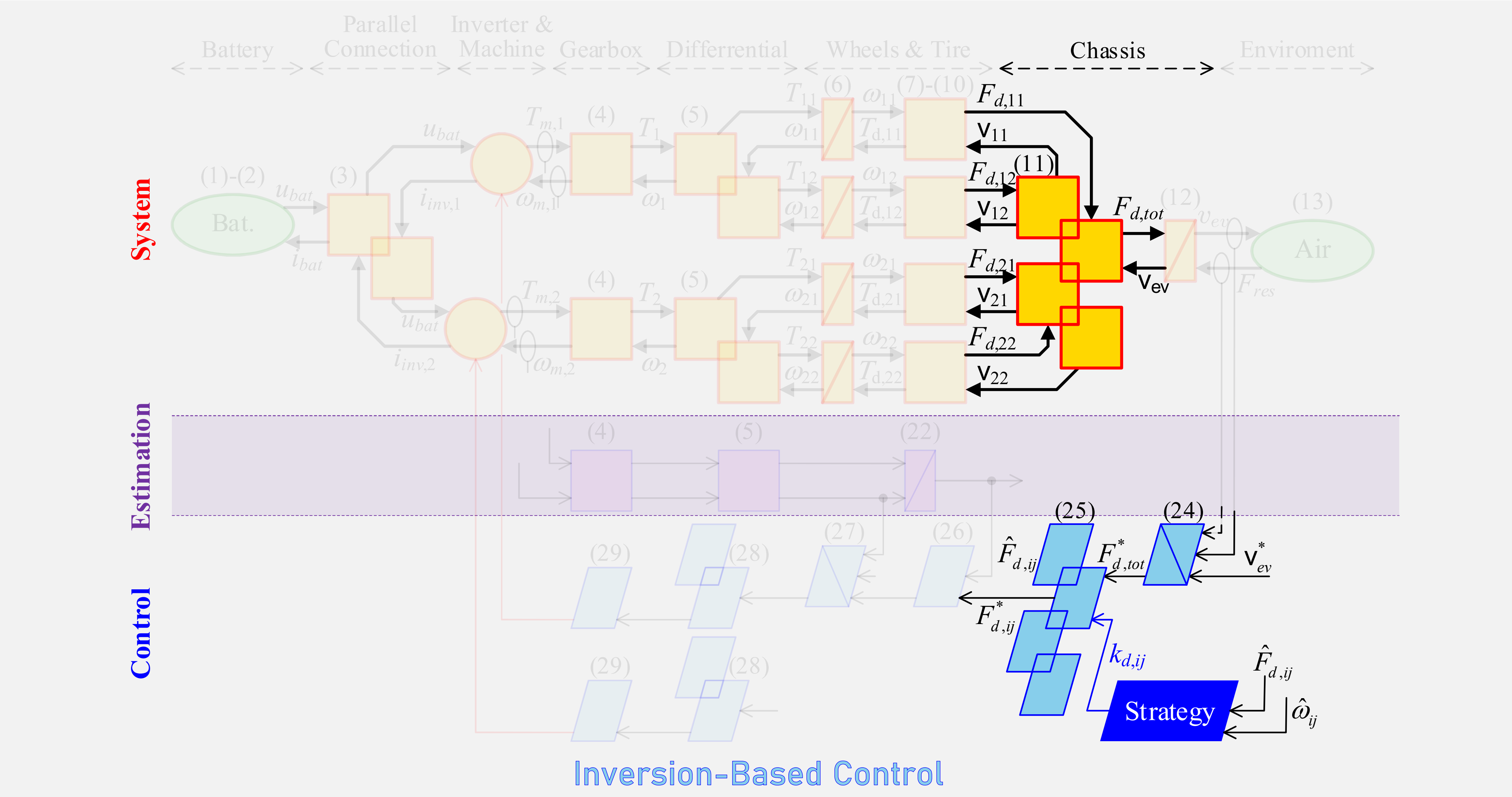

3) Equivalent dynamic equation for each wheel

$$\omega_{ij}^{*} = \frac{R_{wh,ij}}{\widetilde{J}_{\omega,ij}} \int_{0}^{t} (F_{d,ij}^{*} - \hat{F}_{d,ij}) \mathrm{d}t \qquad (26)$$

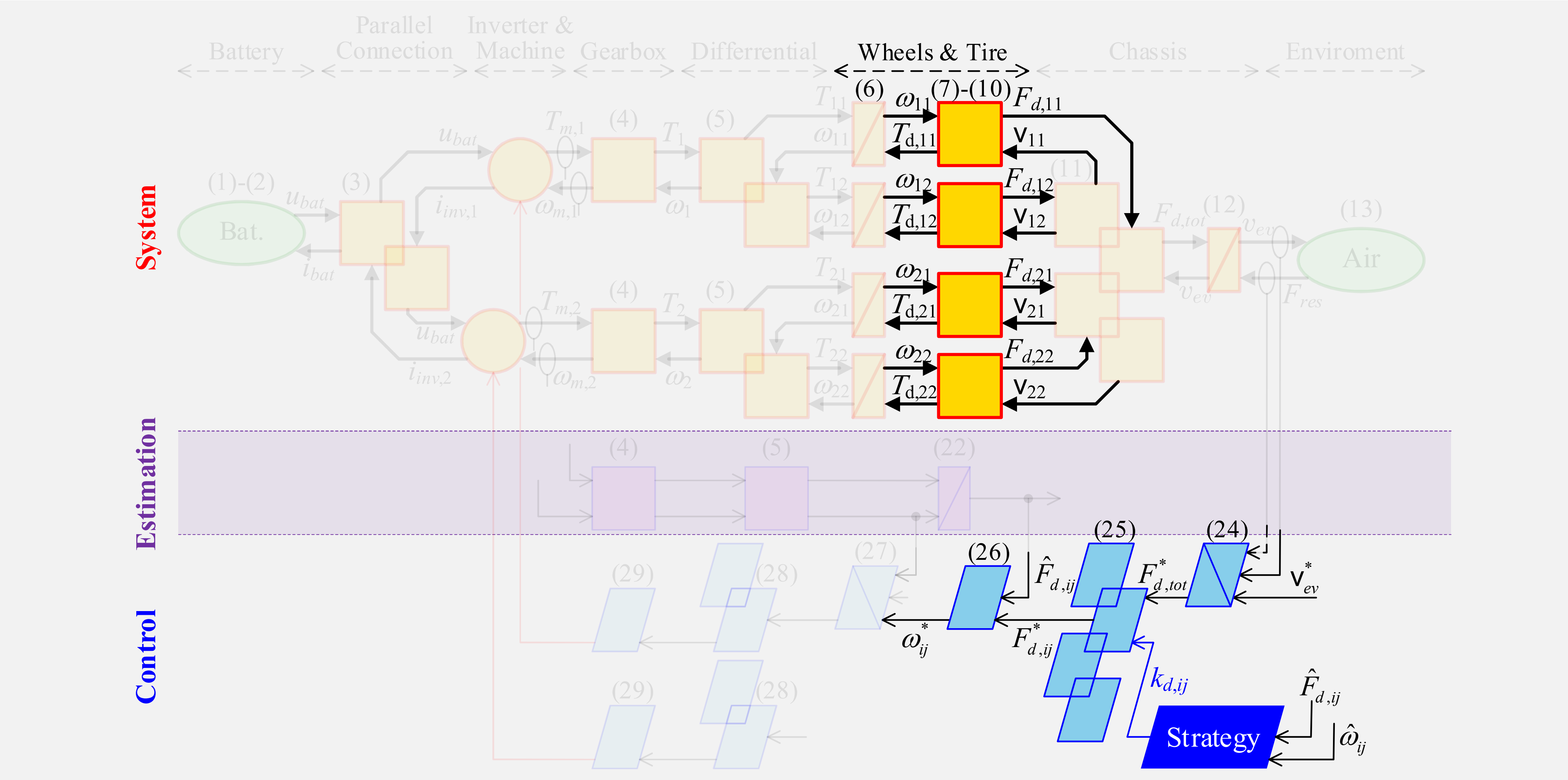

Inversion-Based Control

4) PI angular speed controller

$$T_{ij}^{*} = R_{wh,ij}\hat{F}_{d,ij} + k_{I,\omega}\int_{0}^{t}(\omega_{ij}^{*} - \omega_{ij})\mathrm{d}t + k_{P,\omega}(\omega_{ij}^{*} - \omega_{ij}) \quad (27)$$

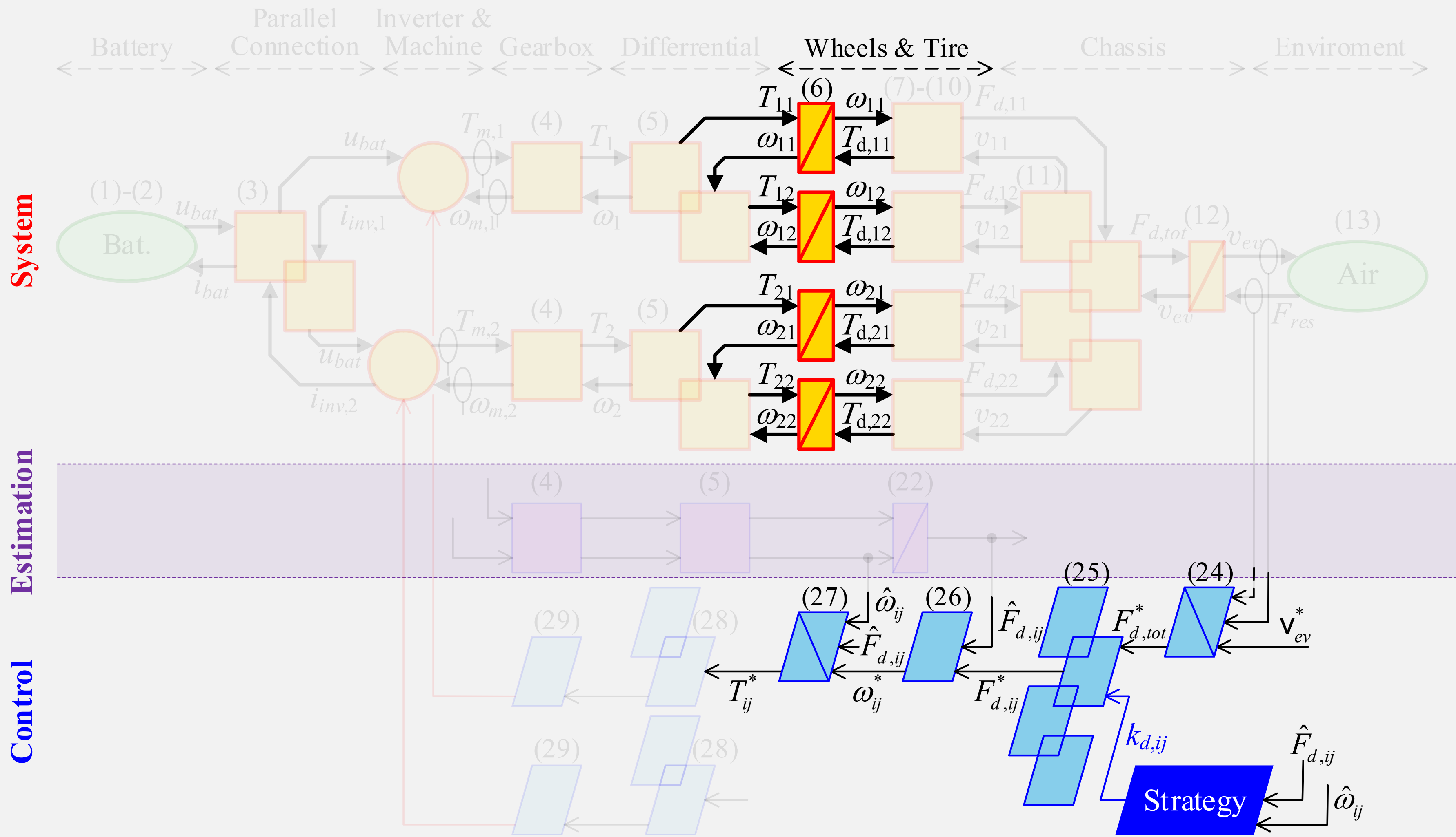

Inversion-Based Control

5) Observers of driving forces

$$\hat{F}_{d,ij} = \left(\hat{T}_{ij} - \mathrm{s}\widetilde{J}_{\omega,ij}\hat{\omega}_{ij}\right)\frac{1}{R_{wh,ij}} \cdot \frac{1}{\tau \mathrm{s}+1} \qquad (22)$$

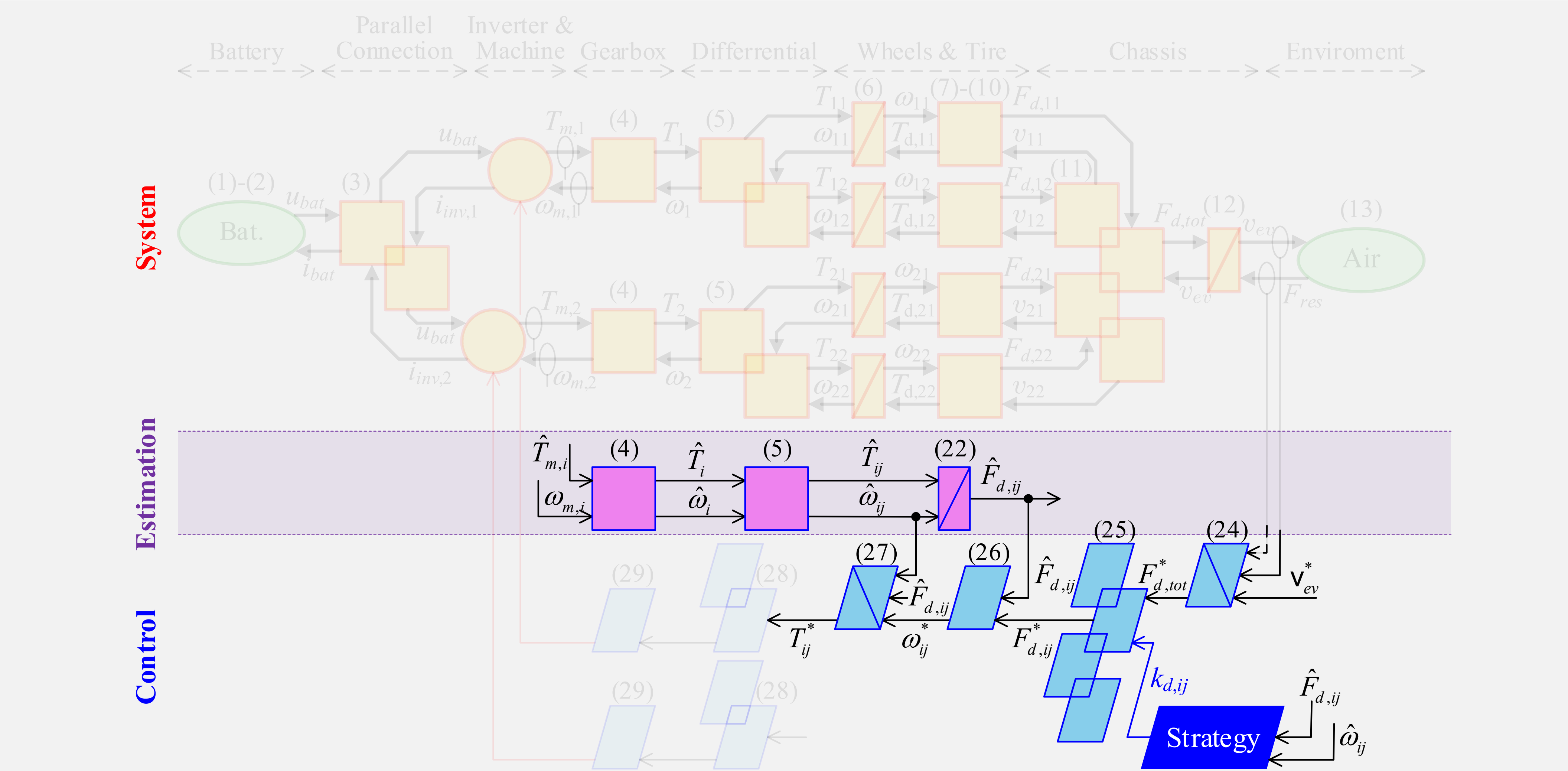

Inversion-Based Control

6) Reference torque of each motor

$$T_i^* = k_{dif,ij}^{-1} T_{ij}^* \qquad (28) \qquad\qquad T_{m,i}^* = k_{gb,i}^{-1} T_i^* \qquad (29)$$

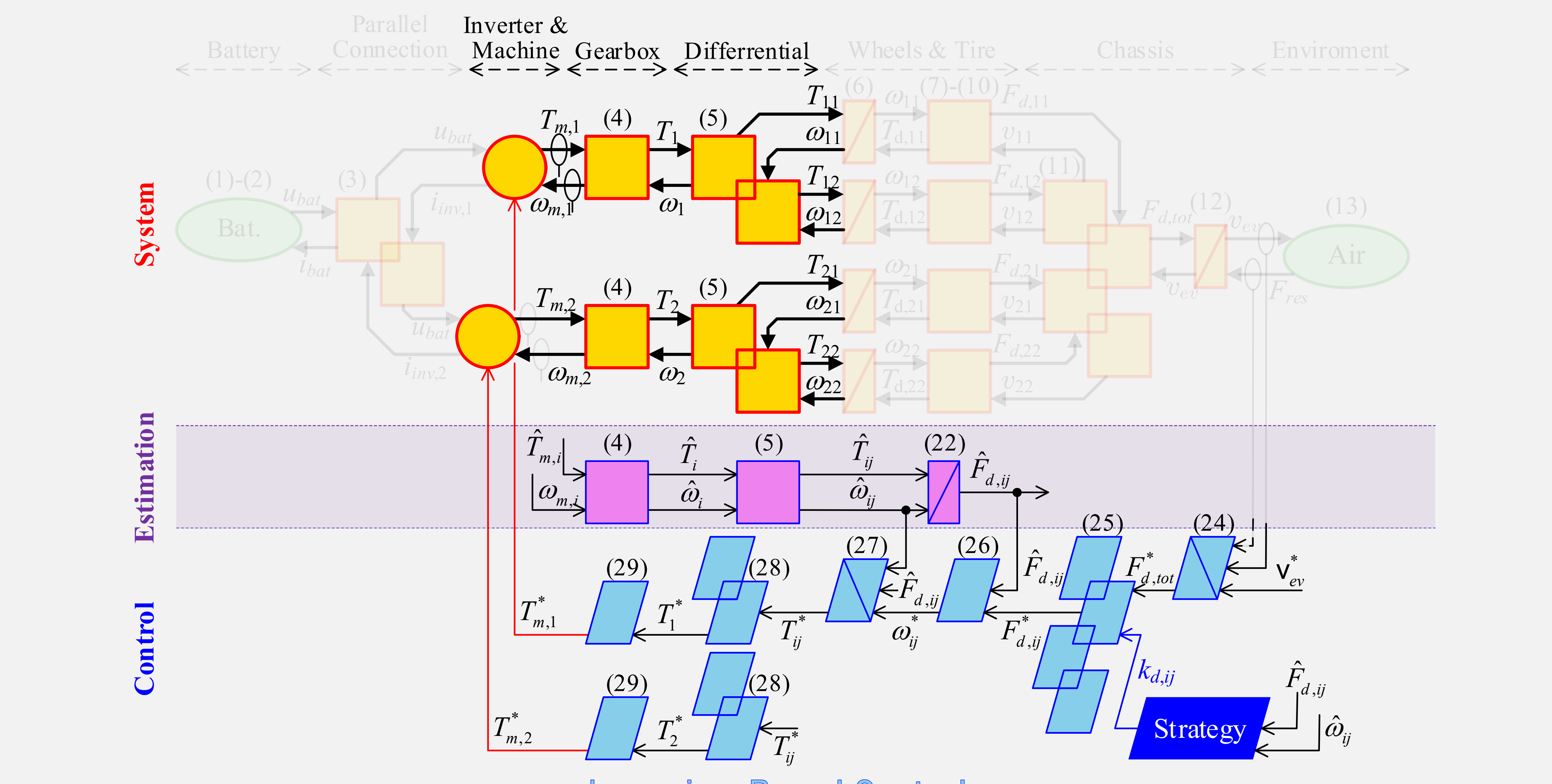

Inversion-Based Control

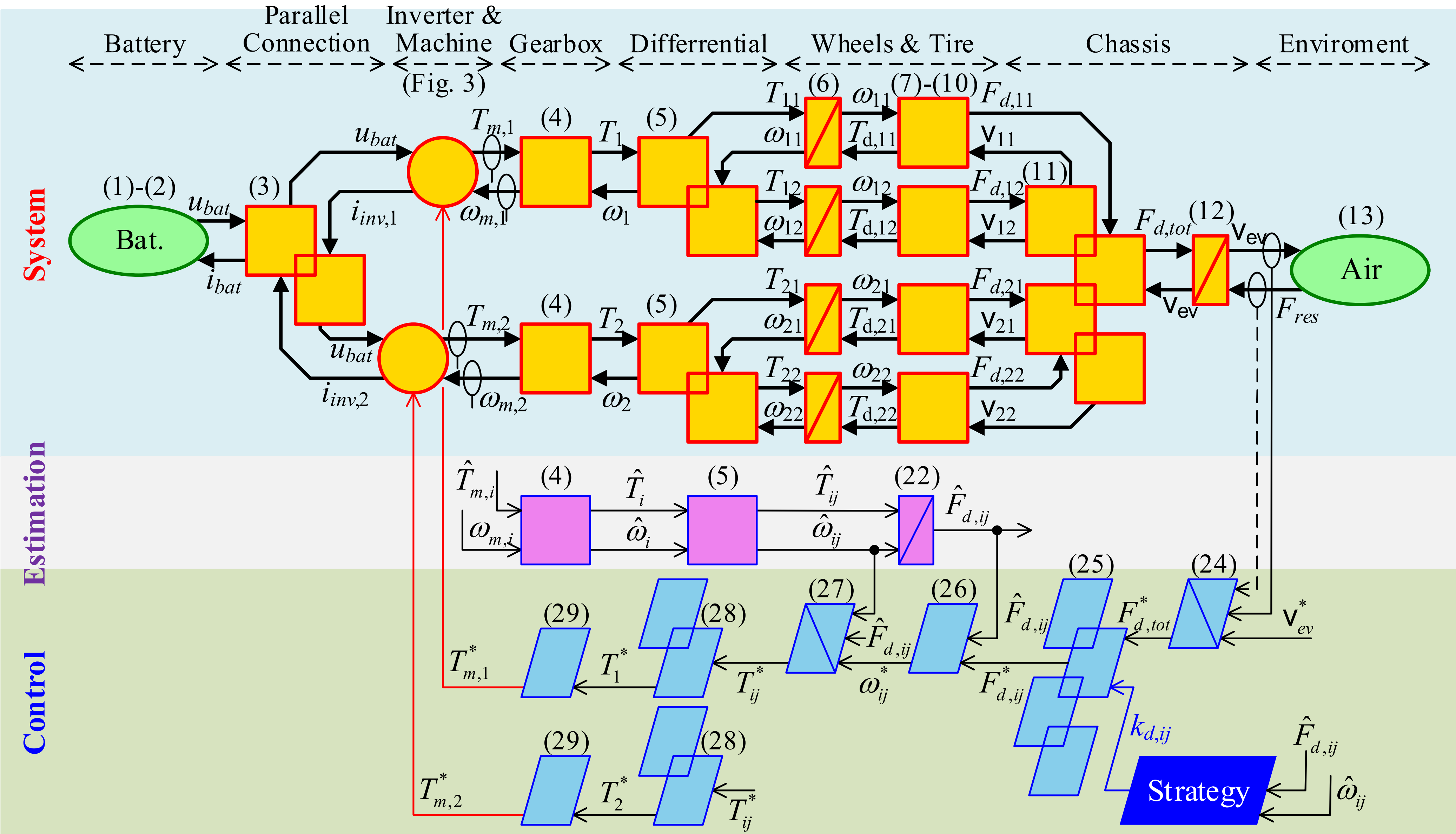

EMR and control scheme of studied vehicle

« SIMULATION »

TABLE. IV
PARAMETERS OF ECOMMANDER PLATFORM

Parameter [Unit]	**Value**
Equivalent vehicle mass m [kg]	857
Height of the center of gravity h_{CG} [m]	0.85
Distance of front axle from CG l_f [m]	0.865
Distance of rear axle from CG l_r [m]	1.058
Front wheels track width of the vehicle d_f [m]	1.257
Rear wheels track width of the vehicle d_r [m]	1.219
Effective radius of tire $R_{w,i}$ [m]	0.318
Equivalent inertia moment of the wheel $\widetilde{J}_{\omega,i}$ [kg $\times$ m^2]	0.55
Drag coefficient c_d	0.65
Equivalent frontal area A_x [m^2]	2

e-Commander at e-TESC Lab.

The studied system is simulated by

MATLAB® & SIMULINK®

Speed profile is a part of the new European driving cycle test.

Speeds of the studied vehicle and the wheels

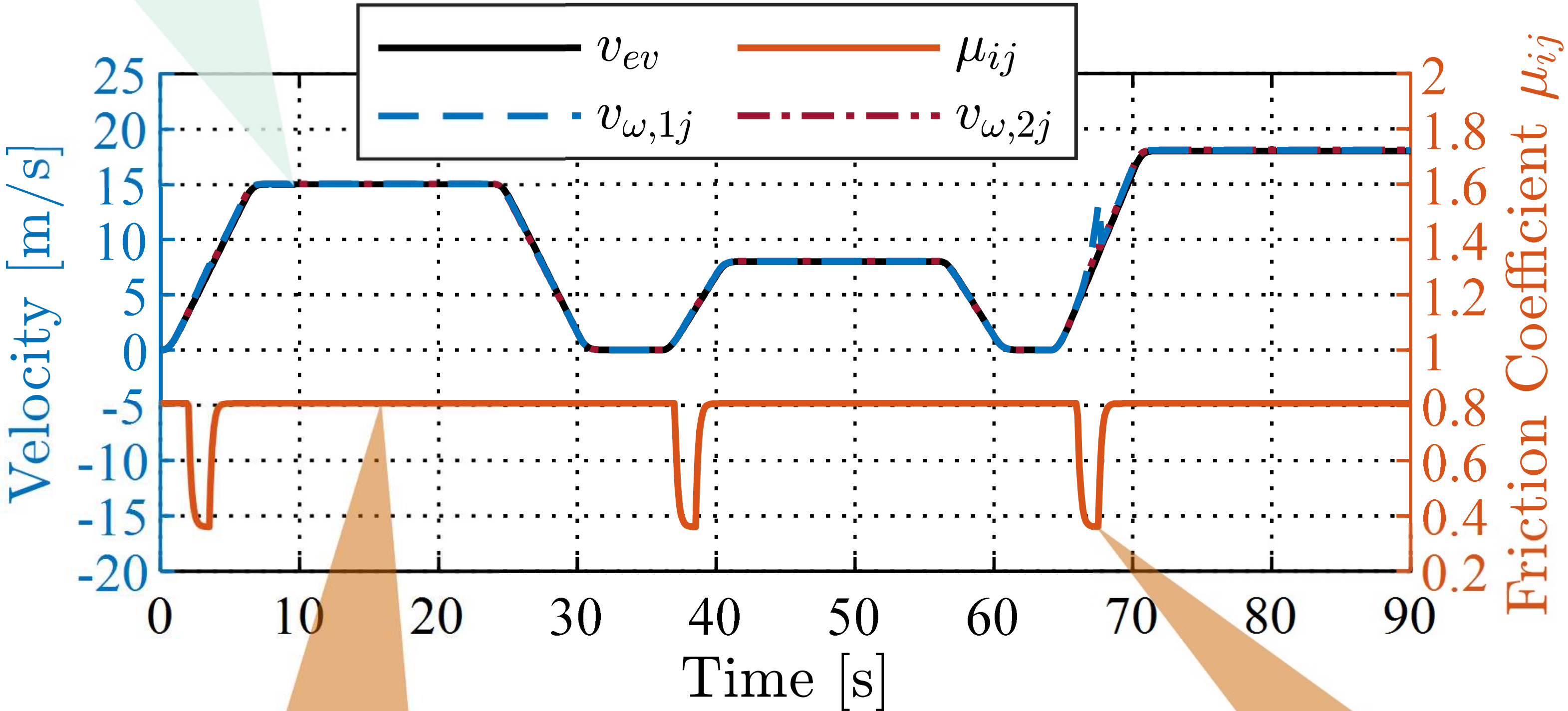

High value of the road friction coefficient (0.8)

Low value of the road friction coefficient (0.36)

Scenario

Road friction coefficient was low in the middle of the acceleration stages.

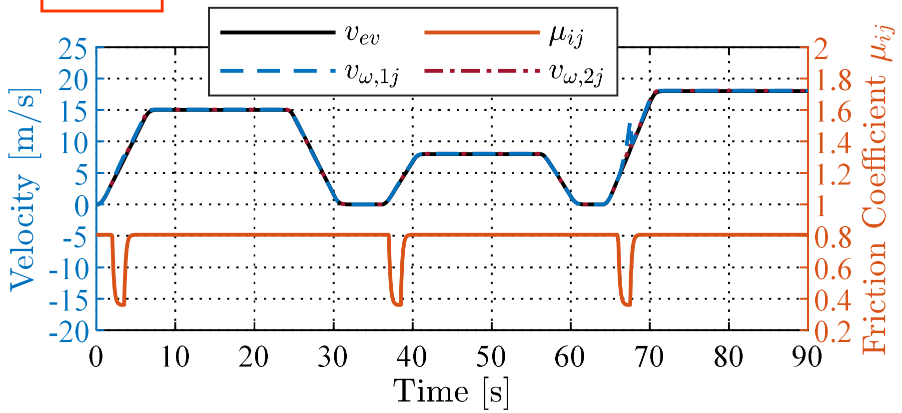

Wheel traction forces of the front axle

- Increase when the EV accelerates.
- Negative value when the EV decelerates.

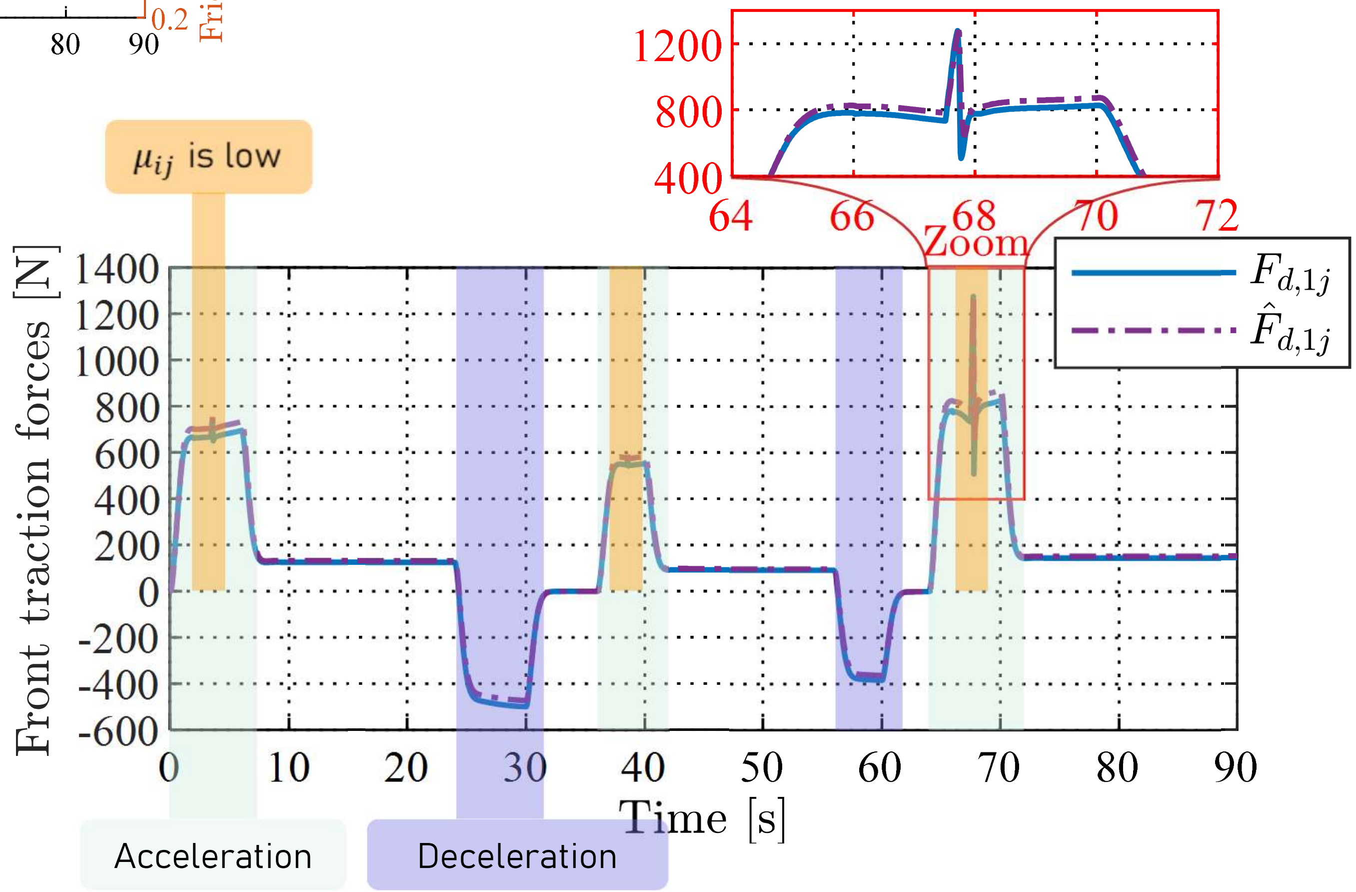

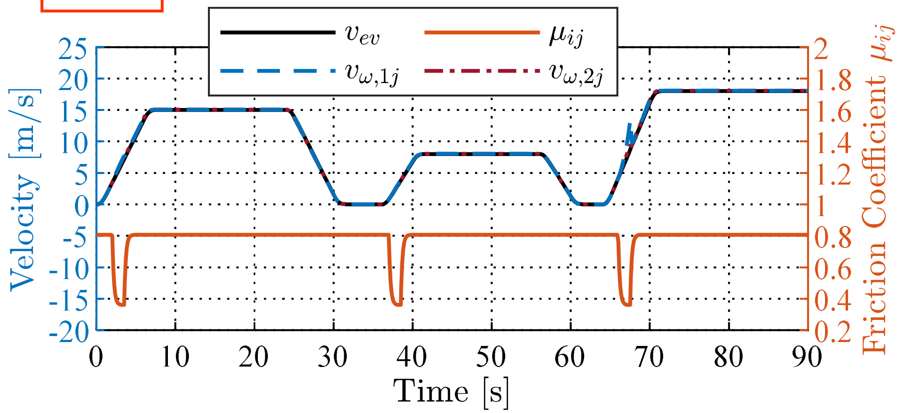

Wheel traction forces of the rear axle

- Increase when the EV accelerates.
- Negative value when the EV decelerates.

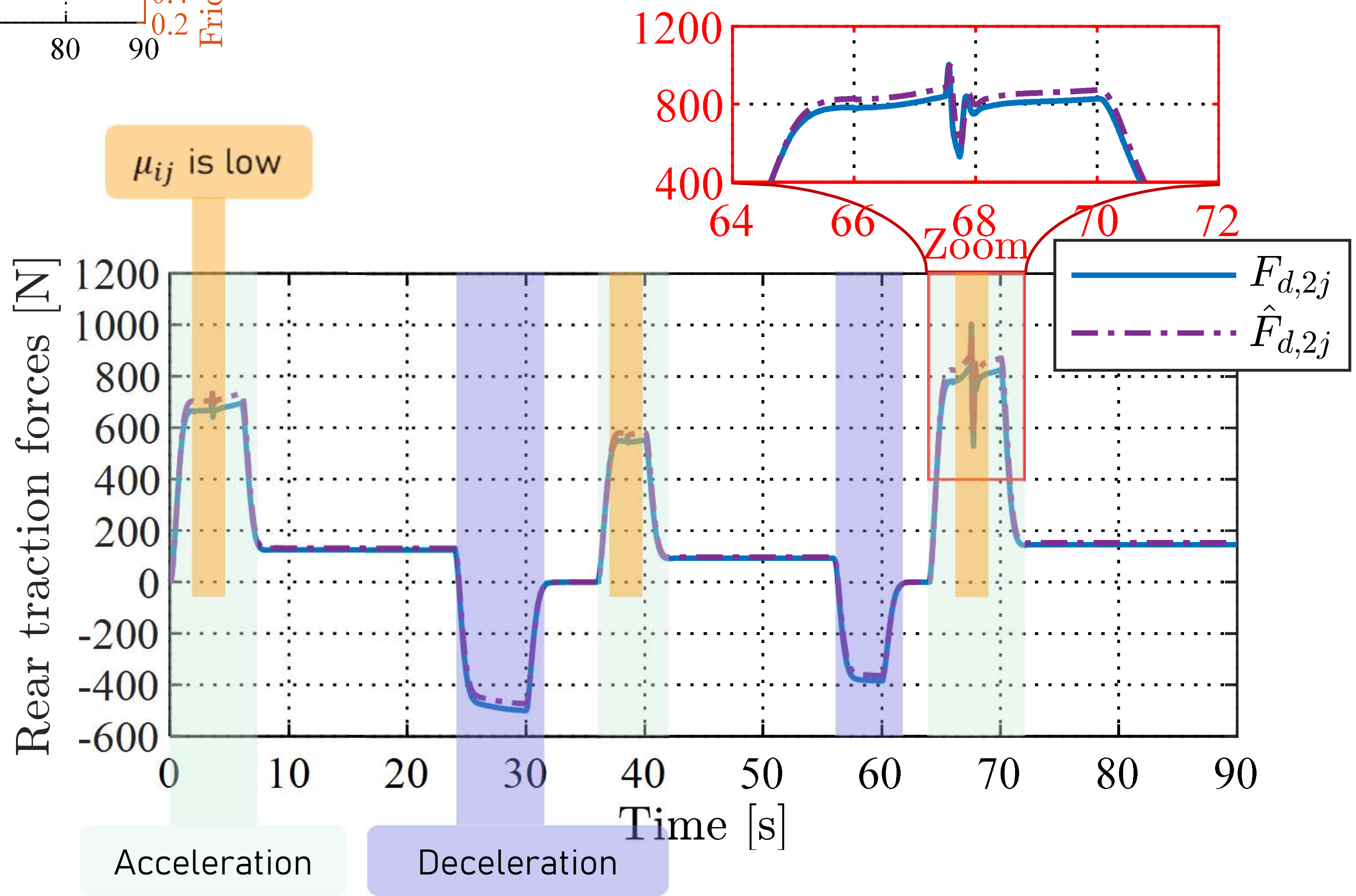

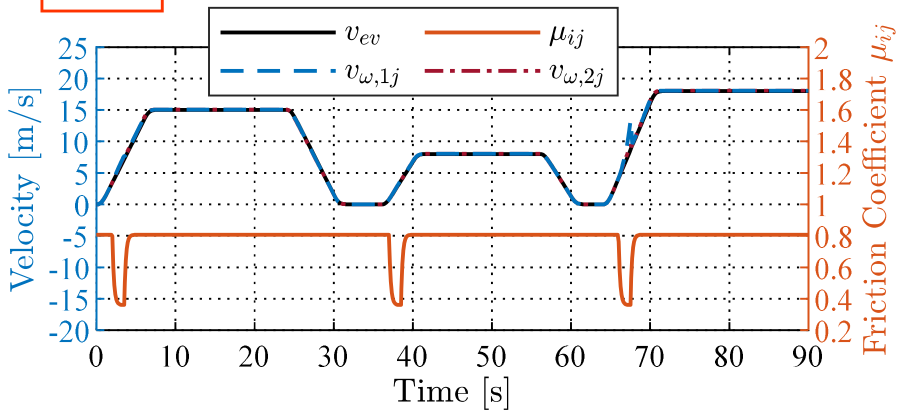

$$\text{Slip ratio } \lambda_{ij} = \frac{R_{wh}\omega_{ij} - v_{ev}}{\max(R_{wh}\omega_{ij}, v_{ev}, \varepsilon)}$$

Slip ratio of the wheels

Increase suddenly if the vehicle is accelerated on a slippery road surface.

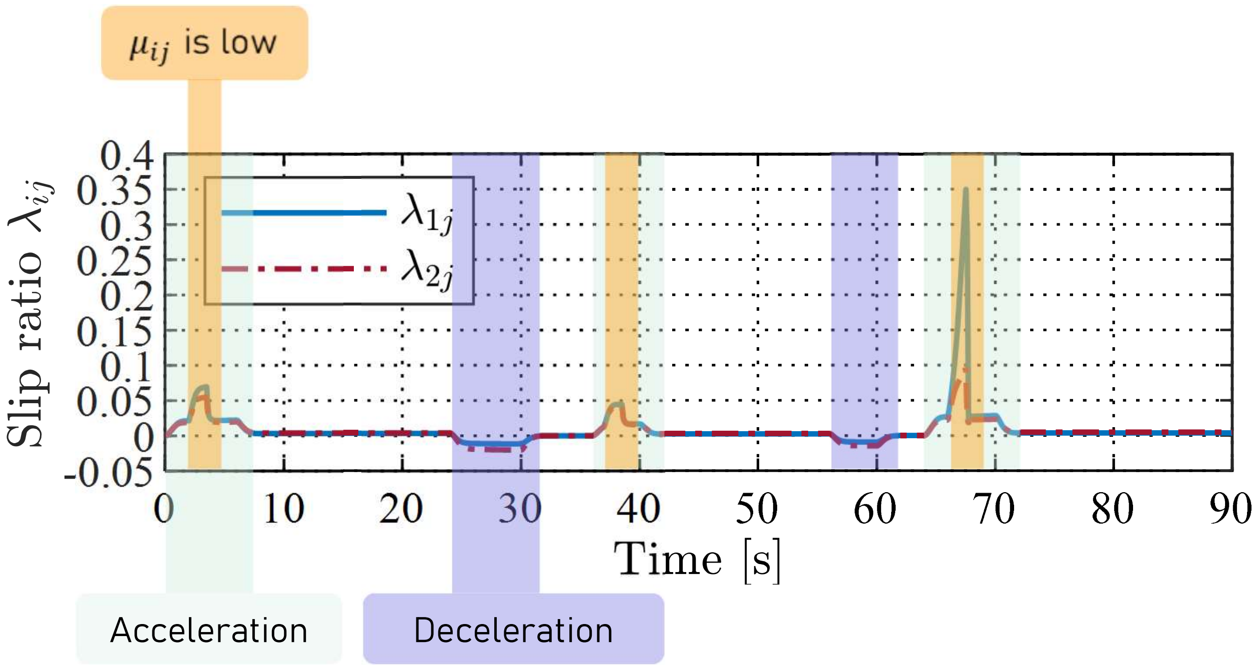

↳ The model of the studied system is similar to the real-world operation of an EV

« CONCLUSION »

Summary

- Studied a dual-motor all-wheel drive EV
- Modelling and control design using EMR
- Simulation in MATLAB/Simulink with NEDC and varied road friction coefficient.

Future Works

Validated by results comparison with commercial software and experiments

Develop different motion control techniques.

Thank you
for your kind attention!

« BIOGRAPHIES AND REFERENCES »

EMR and Control of a Dual-Motor Electric Vehicles

- Authors -

An-Toan NGUYEN, Ph.D. student at the e-TESC Laboratory,
Université de Sherbrooke, Sherbrooke, QC, Canada.
Lecturer in Quy Nhon University, Vietnam.
Research topics: motion control of EVs
An.Toan.Nguyen@USherbrooke.ca

Dr. Binh-Minh NGUYEN, Asst. Prof., University of Tokyo, Tokyo, Japan
Associate Editor of the IEEE Vehicular Technology Magazine
Research topics: glocal control, passivity control, motion control, and their applications in electric vehicles, flying vehicles, and power systems.
nguyen.binhminh@edu.k.u-tokyo.ac.jp

Prof. João TROVÃO, University of Sherbrooke, e-TESC Lab., Canada
IPC-ISEC and INESC Coimbra. Chair of the IEEE-VPPC 2018
Ph.D. in Electrical Engineering at University of Coimbra (2013)
Senior Editor of the IEEE Vehicular Technology Magazine
Research topics: electric vehicles, hybridized energy storage systems, energy management and rotating electrical machines.
Joao.Trovao@USherbrooke.ca

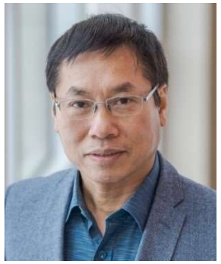

Prof. Minh C. TA, University of Sherbrooke, e-TESC Lab., Canada
Chair of the IEEE-VPPC 2019
Ph.D. in Electrical Engineering at Laval University, QC, Canada (1998)
Guest Editor of the IEEE Transactions on Vehicular Technology.
Research topics: motor drives, advanced control techniques and their applications for electric vehicles and energy conversion systems.
Cao.Minh.Ta@USherbrooke.ca

- References -

[Nguyen 2023] A.-T. Nguyen, B.-M. Nguyen, J. P. F. Trovão, M. C. Ta, "Modelling and Control of Dual-Motor All-Wheel Drive Electric Vehicles using Energetic Macroscopic Representation", *Proceedings of the Canadian Society for Mechanical Engineering International Congress (CSME - CFD-SC2023),* May 2000.

[Nguyen 2015] B.-H. Nguyen, D. Nguyen, V. D. Thanh, and M. C. Ta, "An EMR of Tire-Road Interaction Based-On Magic Formula for Modeling of Electric Vehicles," 2015 IEEE Vehicle Power and Propulsion Conference, 2015.

[Bouscayrol 2023] A. Bouscayrol, B. Lemaire-Semail, "Energetic Macroscopic Representation and Inversion-Based Control ", Encyclopedia of electrical and electronic power engineering, Vol. 3, pp 365-375, Elesevier, DOI : 10.1016/B978-0-12-821204-2.00117-3, ISBN : 978-0-12-823211-8, 2023

[Nguyen 2020] C. T. P. Nguyen, B-H. Nguyen, J. P. F. Trovão, and M. C. Ta, "Effect of battery voltage variation on electric vehicle performance driven by induction machine with optimal flux-weakening strategy," IET Electr. Syst. Transp., vol. 10, no. 4, pp. 351-359, Dec. 2020.